Mn substitution-modified polar phase in the $Bi_{1-x}Nd_xFeO_3$ multiferroics

V. A. Khomchenko' , D. V. Karpinsky, L. C. J. Pereira, A. L. Kholkin, and J. A. Paixão

Citation: Journal of Applied Physics **113**, 214112 (2013); doi: 10.1063/1.4810764
View online: http://dx.doi.org/10.1063/1.4810764
View Table of Contents: http://aip.scitation.org/toc/jap/113/21
Published by the American Institute of Physics

JOURNAL OF APPLIED PHYSICS **113**, 214112 (2013)

Mn substitution-modified polar phase in the $Bi_{1-x}Nd_xFeO_3$ multiferroics

V. A. Khomchenko,[1,a)] D. V. Karpinsky,[2] L. C. J. Pereira,[3] A. L. Kholkin,[2] and J. A. Paixão[1]
[1]*CEMDRX/Department of Physics, University of Coimbra, P 3004 516 Coimbra, Portugal*
[2]*CICECO/Department of Materials and Ceramic Engineering, University of Aveiro, P 3810 193 Aveiro, Portugal*
[3]*Unidade de Ciências Químicas e Radiofarmacêuticas, IST/CTN, Instituto Superior Técnico, Universidade Técnica de Lisboa/CFMCUL, P 2686 953 Sacavém, Portugal*

(Received 23 April 2013; accepted 27 May 2013; published online 7 June 2013)

Room-temperature crystal structure and multiferroic properties of the $Bi_{0.92}Nd_{0.08}Fe_{1-x}Mn_xO_3$ ($x \leq 0.3$) ferromanganites have been studied to reveal the effect of Mn doping on the magnetic and ferroelectric behaviors of the lanthanide-modified compound representing a polar (space group $R3c$) predominantly antiferromagnetic phase of the $Bi_{1-x}Ln_xFeO_3$ perovskites. *B*-site substitution tends to suppress existing polar displacements and induces a ferroelectric-to-antiferroelectric transition near $x = 0.2$. The threshold concentration inducing the structural transformation does not coincide with that required to change the dominant magnetic interaction, so a weak ferromagnetic/ferroelectric state unusual for the $Bi_{1-x}Ln_xFeO_3$ and $BiFe_{1-x}Mn_xO_3$ series appears in the intermediate concentration range near the polar/nonpolar phase boundary. © *2013 AIP Publishing LLC*. [http://dx.doi.org/10.1063/1.4810764]

I. INTRODUCTION

Perovskite-like compounds (general formula ABO_3) are widely known nowadays as materials demonstrating many attractive physical phenomena (e.g., high-temperature superconductivity, colossal magnetoresistance, coexistence of ferroelectricity and magnetism). The latter, having potential for numerous technological applications related to the magnetoelectric effect, becomes one of the main topics of the condensed matter research.[1–3] Among multiferroic perovskites, $BiFeO_3$ is distinguished by the broadest temperature range of a spin and electric dipole ordering coexistence ($T_{AF} \approx 640$ K, $T_{FE} \approx 1100$ K).[3] At room temperature, bismuth ferrite possesses a rhombohedral structure (space group $R3c$) compatible with the spontaneous polarization ($P_s \sim 100\ \mu C/cm^2$)[4,5] directed along the $[001]_{hex}$ axis.[6,7] The ferroelectricity is caused by the stereochemically active Bi^{3+} cations containing a highly polarizable 6*s* lone pair of valence electrons that demonstrate a strong tendency to break a local inversion symmetry.[8] Though superexchange interactions Fe^{3+} O Fe^{3+} alone would give rise to a *G*-type antiferromagnetic (AF) alignment of the iron magnetic moments in $BiFeO_3$,[9,10] a coupling between the ferroelectric and magnetic subsystems stabilizes a more complicated magnetic structure with a long-range (~620 Å) cycloidal modulation.[11] This modulation eliminates any spontaneous magnetization which could be induced by the Dzyaloshinsky-Moriya interaction[12] to make impossible controlling the ferroelectric subsystem of $BiFeO_3$ via a moderate magnetic field application. It has been recognized that *A*-site lanthanide (*Ln*) substitution increases magnetic anisotropy in bismuth ferrite to make spatial modulation energetically unfavorable.[13,14] Though earlier publications devoted to multiferroic properties of the $Bi_{1-x}Ln_xFeO_3$ perovskites suggest the possibility to combine weak ferromagnetism and ferroelectricity in the lanthanide-modified phases,[15] more recent works do not support this assumption and indicate that the doping-driven suppression of the cycloidal modulation resulting in the establishment of weak ferromagnetic (wF) state is accompanied by the destruction of the initial polar structure, maximum magnetization in the $Bi_{1-x}Ln_xFeO_3$ series ($M_s \sim 0.25$ 0.3 emu/g) being achieved only in the substitution-stabilized nonpolar phases [upon lanthanide substitution, the initial ferroelectric rhombohedral ($R3c$) AF phase typically transforms into the intermediate antiferroelectric orthorhombic (*Pnam* for *Ln* = Pr, Nd, Sm[16–18] or *Pnam* and *Imma*$(00\gamma)s00$ for *Ln* = La[19,20]) wF phase that, in turn, transforms into nonpolar orthorhombic (*Pnma*) wF phase characteristic of $LnFeO_3$ orthoferrites]. Decreasing ionic radius of a substituting lanthanide shifts phase boundaries of the doping-induced transitions toward smaller *x* (for the $R3c \rightarrow Pnam$ phase transition, the critical concentration varies from ~18% for *Ln* = La[19,20] to ~14% for *Ln* = Sm[18]). In contrast to the lanthanide-modified systems, the $BiFe_{1-x}Mn_xO_3$ compounds keep the initial polar structure unaltered and do not exhibit weak ferromagnetic behavior in the entire concentration range of the solid solutions realization (i.e., at $x \leq 0.3$ for the ambient-pressure synthesis).[21,22] Effect of combined *Ln*/Mn substitution (*Ln* = La,[23] Pr,[24] Nd,[25] and Sm[26–28]) on the crystal structure and magnetization behavior of the $BiFeO_3$ perovskite has also been recently studied; however, these investigations, being mainly focused on aspects related to doping-induced structural transformations in the (Bi, *Ln*)$Fe_{1-x}Mn_xO_3$ series (depending on chemical composition, manganese substitution can stabilize both commensurate and incommensurate nonpolar structures[23–28]), do not give a clear understanding how Mn doping influences multiferroic properties of the $Bi_{1-x}Ln_xFeO_3$ compounds in the initial polar phase. To contribute to answering this question, a detailed analysis of crystal structure,

a)Author to whom correspondence should be addressed. Electronic mail: uladzimir@fis.uc.pt. Telephone: +351 239 410 637. Fax: +351 239 829 158.

ferroelectric, and magnetic properties of the $Bi_{0.92}Nd_{0.08}Fe_{1-x}Mn_xO_3$ compounds (in the $Bi_{1-x}Nd_xFeO_3$ series, the ferroelectric-to-antiferroelectric phase transition takes place within the range $0.1 < x < 0.15$ (Ref. 17)) was carried out. A doping-driven decoupling of the antiferromagnetic-weak ferromagnetic and ferroelectric-antiferroelectric transitions resulting in the appearance of a weak ferromagnetic polar phase uncommon for $Bi_{1-x}Ln_xFeO_3$ and $BiFe_{1-x}Mn_xO_3$ perovskites was found.

II. EXPERIMENTAL

Polycrystalline samples of $Bi_{0.92}Nd_{0.08}Fe_{1-x}Mn_xO_3$ ($x \leq 0.3$) were prepared by a conventional solid-state reaction method using the high-purity oxides Bi_2O_3, Nd_2O_3, Fe_2O_3, and Mn_2O_3. The reagents were taken in stoichiometric cation ratio, mixed and pressed into pellets. The synthesis was carried out in air at 870 °C for 15 h to yield ceramic materials with the grain size distributed in the range from 1 to 5 μm [inset in Fig. 1; the backscattered-electron image was obtained with a Phenom G2 pro desktop scanning electron microscope (Phenom-World)]. X-ray diffraction (XRD) patterns were collected at room temperature using a Rigaku D/MAX-B diffractometer with Cu K_α radiation. The data were analyzed by the Rietveld method using the FullProf program.[29] Local ferroelectric properties were investigated with piezoresponse force microscopy (PFM) using a commercial setup NTEGRA Prima (NT-MDT). A commercial NANOSENSORS™ PPP-NCHR probe with a resonance frequency around 300 kHz was used. Domain visualization was performed under an applied *ac* voltage with an amplitude $V_{ac} = 4.5$ V and frequency $f = 100$ kHz. Local poling was done by applying a *dc* bias between the tip and the counter electrode, followed by subsequent PFM imaging. Local piezoelectric hysteresis loops were measured inside individual grains by applying the consecutive voltage pulses and measuring the piezoelectric response as a function of the voltage. Magnetic measurements were performed with a superconducting quantum interference device (SQUID) magnetometer (S700X, Cryogenic Ltd).

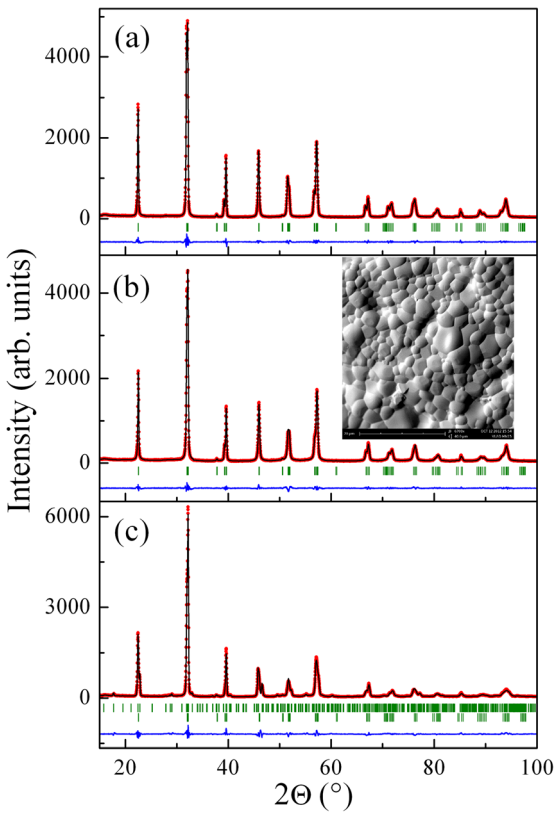

FIG. 1. Observed, calculated, and difference X ray diffraction patterns obtained for the $Bi_{0.92}Nd_{0.08}Fe_{1-x}Mn_xO_3$ (x 0.1 (a), x 0.15 (b), and x 0.2 (c)) compounds at room temperature. The antiferroelectric phase of the phase separated x 0.2 sample was described in the approximation of commensurate orthorhombic structure with the space group *Pbam* (see Refs. 19, 20, 22 26 for more details). Inset shows backscattered electron image of the $Bi_{0.92}Nd_{0.08}Fe_{0.85}Mn_{0.15}O_3$ ceramics.

III. RESULTS AND DISCUSSION

X-ray diffraction patterns obtained for the $Bi_{0.92}Nd_{0.08}Fe_{1-x}Mn_xO_3$ ($x = 0$, 0.05, 0.1 and 0.15) compounds at room temperature were successfully fitted using the structural model characteristic of pure bismuth ferrite.[6,7] Indeed, the diffraction peaks were indexed using the hexagonal $\sqrt{2}a_c \times \sqrt{2}a_c \times 2\sqrt{3}a_c$ cell ($a_c \sim 4$ Å is the parameter of the primitive cubic perovskite subcell) to give the extinctions consistent with the space group $R3c$ (Figs. 1(a) and 1(b)). Initially, the randomly distributed Bi/Nd and Fe/Mn cations were suggested to occupy the 6a (00z) sites with $z = 0$ (fixed as origin of coordinates) and $z \approx 0.25$, respectively. Oxygen anions occupy the general position site 18b with $x \approx 0.5$, $y \approx 0$, and $z \approx 1$ (Fig. 2(a)). The model was treated with the FULLPROF software package to yield the refined structure sketched in Fig. 2(b). With respect to the cubic $Pm\bar{3}m$ lattice peculiar to an ideal perovskite, structural distortions in the rhombohedral phase can be described in terms of the antiphase tilting of the adjacent oxygen octahedra ($a^-a^-a^-$ tilt system in Glazer's notation[30]) and the polar ionic displacements along the $\langle 111 \rangle_c$ direction of the parent cubic cell ($[001]_{hex}$ direction in the hexagonal setting) (Fig. 2). The refined structural data (an example is shown in Table I) were used to analyze compositional dependence of the ferroelectric polarization in the system under study. Spontaneous polarization appearing as a result of the ionic rearrangements can be calculated as

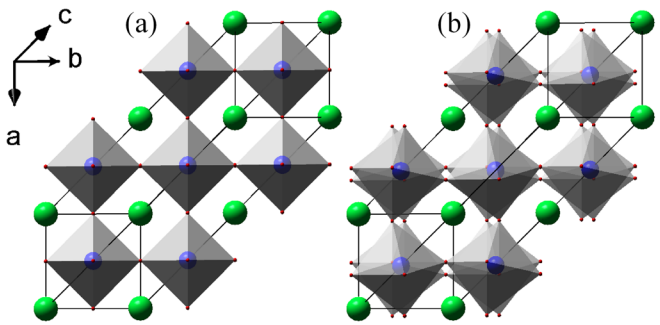

FIG. 2. Atomic arrangement in the "$Pm\bar{3}m$" (a) and "$R3c$" (b) structures along the axis coincident with one of the $\langle 100 \rangle_c$ directions of the parent cubic perovskite cell. Representation of the rhombohedral structure is based on the refined parameters obtained for the $Bi_{0.92}Nd_{0.08}Fe_{0.9}Mn_{0.1}O_3$ compound (Table I).

TABLE I. Structural parameters of the $Bi_{0.92}Nd_{0.08}Fe_{0.9}Mn_{0.1}O_3$ compound at room temperature (space group $R3c$).

Cell (Å)		Atom	Site	x	y	z	$U_{iso} \times 100$ (Å^2)	R factors (%)	
a 5.5704(1) c	13.7845(2)	Bi/Nd	6a	0	0	0	2.02(2)	R_p	5.26
		Fe/Mn	6a	0	0	0.22449(20)	1.25(7)	R_{wp}	6.71
		O	18b	0.4360(16)	0.0012(16)	0.9609(5)	1.6(2)	R_B	5.08

$$P_s = \sum_i (m_i \Delta x_i Q_i) e/V,$$

where m_i is the crystallographic site multiplicity, Δx_i is the ionic displacement along the polar axis from the corresponding position in the paraelectric phase, and $Q_i e$ is the formal charge of the ith ion located in the unit cell volume V. The low-doped ($x \leq 0.15$) air-prepared (Bi,Ln)$Fe_{1-x}Mn_xO_3$ compounds do not possess a large oxygen nonstoichiometry,[21–24] so its effect on the point-charge polarization value was neglected. Suppression of both Fe/Mn and O displacements is observed with increasing Mn content, and the calculated polarization decreases from $\sim 64\,\mu C/cm^2$ for $x = 0$ to $\sim 53\,\mu C/cm^2$ for $x = 0.15$ (Fig. 3). The decrease and, eventually, disappearance of the spontaneous polarization associated with the dilution of the Bi sublattice is a quite natural scenario characteristic of both isovalent-substituted[31] and heterovalent-substituted[32,33] $Bi_{1-x}A_xFeO_3$ multiferroics. Comparison of concentration ranges of the polar phase development in the $Bi_{1-x}Ln_xFeO_3$ series[16–20] implies that the difference between ionic radii of the host and doping elements is a key factor controlling the effect of chemical substitution on the ferroelectric properties of the modified $BiFeO_3$ (decreasing tolerance factor $t = \frac{r_A + r_O}{\sqrt{2}(r_B + r_O)}$, where r_A, r_B, and r_O are the ionic radii of A, B, and O ions; $r_{Ln^{3+}} < r_{Bi^{3+}}$ (Ref. 34) shifts phase boundary of the polar-nonpolar transition towards smaller x). Despite the opposite influence of the Mn doping on the tolerance factor [unit cell volume in the $Bi_{0.92}Nd_{0.08}Fe_{1-x}Mn_xO_3$ series decreases with increasing Mn content (Fig. 3)], the B-site substituents similarly affect the cooperative dipole ordering peculiar to pure $BiFeO_3$. The decrease of spontaneous polarization observed in the $Bi_{0.92}Nd_{0.08}Fe_{1-x}Mn_xO_3$ system should be associated with the local disorder/distortions induced by the Mn substitution and affecting the anisotropic character of the chemical bonds $Bi^{3+}(6s^2)$ O^2 $(2p^6)$. Above $x = 0.15$, Mn doping induces appearance of the incommensurate antiferroelectric phase (Fig. 1(c)), whose crystal structure[19] and multiferroic properties[20,24,26] have been already a subject of the detailed investigations. It is known that ferroelectric-to-antiferroelectric transition in the $BiFeO_3$-based perovskites is accompanied by a change of the BO_6 octahedra tilting scheme[19] and thus can be considered as arising via suppression of polarization by a structural order parameter.[35] While the initial rhombohedral phase coexists with the doping-induced orthorhombic one at $x = 0.2$ (Fig. 1(c)), the $x = 0.25$ and $x = 0.3$ compounds are purely orthorhombic. The Rietveld refinement applied to the rhombohedral phase of the $x = 0.2$ sample gives structural parameters compatible with the spontaneous polarization of $52\,\mu C/cm^2$; however, complexity of the resulting structural model and a relatively small amount of the polar phase in the sample (~30%) leaves some doubts about reliability of this value. Accordingly, the data obtained for the ferroelectric phase of the $x = 0.2$ compound were not included in the compositional dependence of spontaneous polarization (Fig. 3). A ferroelectric nature of the Mn-containing rhombohedral compounds was directly confirmed by the piezoresponse force microscopy measurements, which revealed a clear piezoelectric contrast corresponding to antiparallel domains. An electric-field-induced polarization switching was also found. The measured piezoresponse was comparable with that observed for pure bismuth ferrite. Example of the local measurements performed for the $x = 0.15$ sample containing a close-to-largest amount of the Mn ions allowing the cooperative polar ordering to be kept is shown in Fig. 4. Local ferroelectric properties of the substitution-stabilized antiferroelectric phase were recently investigated in $Bi_{1-x}La_xFeO_3$ ceramics and no distinct piezoresponse was found.[20]

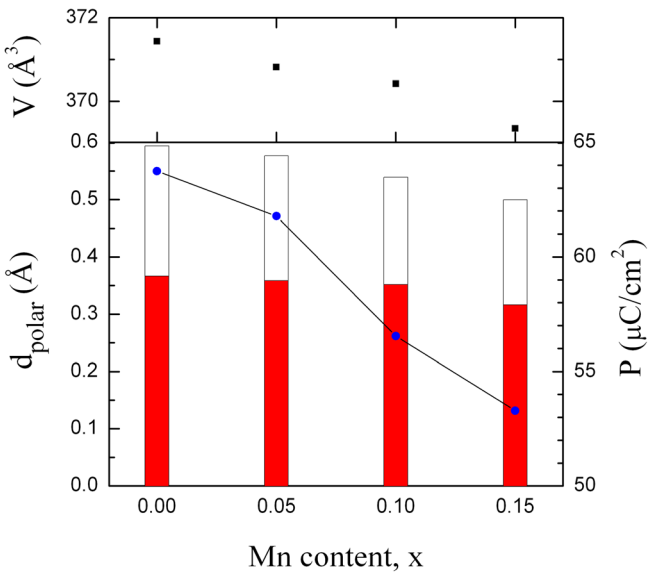

FIG. 3. Concentrational dependences of the unit cell volume (black squares), polarization (blue circles) and polar displacements of the O^2 (white bars) and $\langle Fe/Mn \rangle^{3+}$ (red bars) ions for the single phase rhombohedral $Bi_{0.92}Nd_{0.08}Fe_{1-x}Mn_xO_3$ ($x \leq 0.15$) compounds at room temperature.

Though the present work is mainly aimed at the study of single-phase polar compounds, $0 \leq x \leq 0.15$, magnetic properties of the antiferroelectric samples, $0.2 < x \leq 0.3$, will also be reported below to illustrate main regularities characteristic of the $Bi_{0.92}Nd_{0.08}Fe_{1-x}Mn_xO_3$ system. $BiFeO_3$ belongs to the so-called "type-I" multiferroics, in which ferroelectricity and magnetism appear largely independently of one another.[36] Nevertheless, an inhomogeneous magnetoelectric

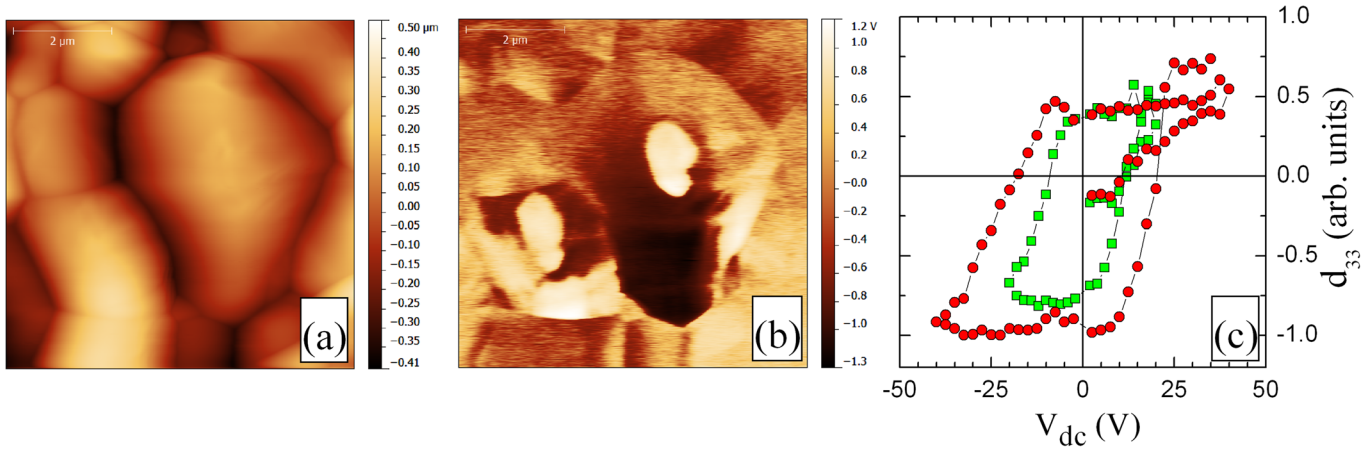

FIG. 4. Scanning probe microscopy measurements of the $Bi_{0.92}Nd_{0.08}Fe_{0.85}Mn_{0.15}O_3$ ceramics: topography (a), electric field induced PFM contrast after poling with V_{dc} 60 V (dark spot) and V_{dc} 60 V (bright spots), and local piezoresponse hysteresis loops obtained from the surface of two different grains (c).

interaction influences both ferroelectric and magnetic subsystems of the material and stabilizes the spatially modulated magnetic structure.[37] The modulated structure can be suppressed by applying a strong magnetic field $H_c \sim 180$ 200 kOe to release a weak ferromagnetic moment of ~0.25 emu/g.[38] In polar phase, lanthanide substitution decreases the critical field H_c (Refs. 13, 14, and 16) and induces a small remanent magnetization of ~0.03 0.05 emu/g.[16,20,39,40] The dominant magnetic state, however, remains antiferromagnetic up to the concentration transition into the antiferroelectric phase.[16,20,39,40] In this phase, the $Bi_{1-x}Ln_xFeO_3$ compounds acquire spontaneous magnetization, whose value is very close to that released upon the magnetic field-induced AF-wF transition.[16,20] $Bi_{0.92}Nd_{0.08}Fe_{1-x}Mn_xO_3$ ($x \leq 0.1$) samples exhibit magnetic properties typical of the rhombohedral $Bi_{1-x}Ln_xFeO_3$ perovskites[16,20,39–41] (Fig. 5(a)). The remanent magnetization is far below the value expected for the homogeneous weak ferromagnetic state and varies in a relatively narrow range from 0.024 emu/g for $x = 0$ to 0.047 emu/g for $x = 0.1$. The situation drastically changes with further increase of the Mn content. Indeed, polar $x = 0.15$ sample demonstrates the field dependence of magnetization characteristic of the $Bi_{1-x}Ln_xFeO_3$ compounds in the doping-induced nonpolar wF phase[16,20,39–41] (Fig. 5(a)). Its spontaneous magnetization, as extracted from the linear extrapolation of the high field magnetization to H = 0, practically coincides with the remanent one (0.106 emu/g). The highest spontaneous magnetization in the $Bi_{0.92}Nd_{0.08}Fe_{1-x}Mn_xO_3$ series (0.124 emu/g) is observed for the $x = 0.2$ sample (i.e., near the morphotropic phase boundary) (Fig. 5(b)). In the substitution-stabilized orthorhombic phase, a gradual decrease of the room-temperature magnetization takes place with increasing Mn concentration (Fig. 5(b)). Similar evolution of the magnetic behavior near the rhombohedral-orthorhombic phase boundary was recently observed for the $Bi_{0.89}Pr_{0.11}Fe_{1-y}Mn_yO_3$ series.[24]

In accordance with the results of the magnetic properties study (Fig. 5), three distinct regions on the compositional dependence of the remanent/spontaneous magnetization in the $Bi_{0.92}Nd_{0.08}Fe_{1-x}Mn_xO_3$ system can be market out (Fig. 6). The low-doped compounds (red dotted region in Fig. 6) retain the dominant AF state and exhibit a very slight increase of the remanent magnetization with increasing Mn content. The behavior is consistent with our previous study,[39] which found that changing the average ionic radius of the *A*-site ions in the $Bi_{0.86}La_{0.14-x}Sm_xFeO_3$ series could have no appreciable effect on remanent magnetization in the concentration range of the polar phase existence. It has been suggested that the local deviation from a homogeneous distribution of the substituting elements typical of perovskite solid solutions[42] or/and lattice defects might be the driving force for the local suppression of the cycloidal magnetic modulation in the rhombohedral phase to induce the appearance of a small remanence.[39] Cooperative removal of the cycloidal structure that would stabilize a purely weak

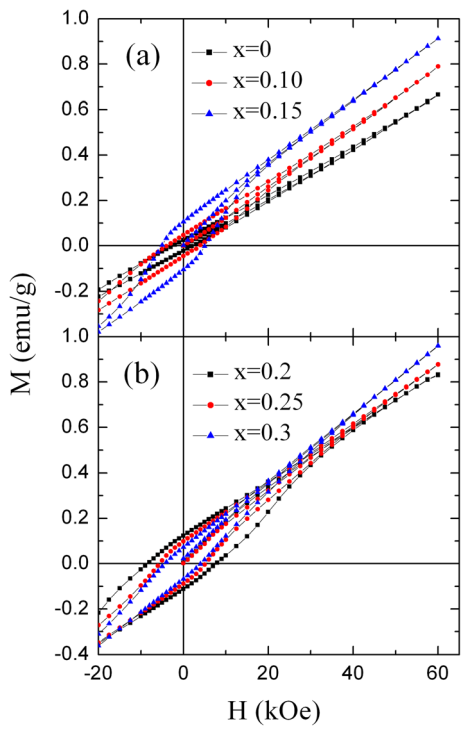

FIG. 5. Field dependences of the magnetization obtained for the $Bi_{0.92}Nd_{0.08}Fe_{1-x}Mn_xO_3$ compounds at room temperature.

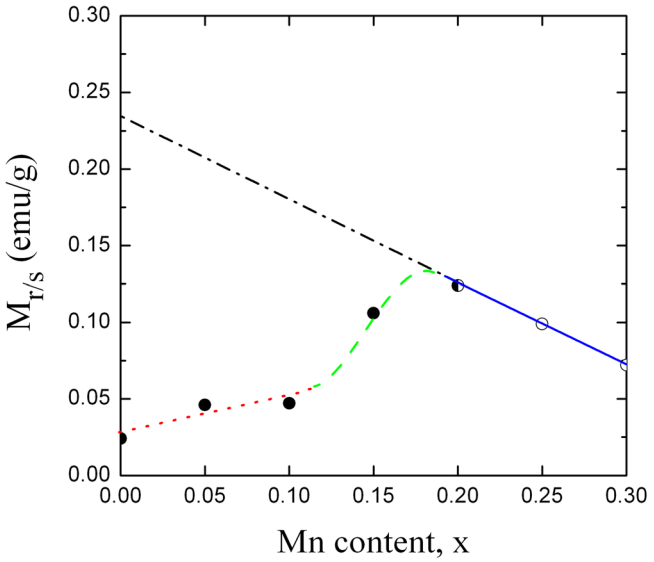

FIG. 6. Compositional dependence of the remanent/spontaneous magnetization for the rhombohedral (close symbols)/orthorhombic (open symbols) compounds of the $Bi_{0.92}Nd_{0.08}Fe_{1-x}Mn_xO_3$ ($x \leq 0.3$) system at room temperature. The color marked regions composing the eye guide curve separate the AF polar phase (red dotted line), wF nonpolar phase (blue solid line), and intermediate polar phase in which the change of the dominant magnetic state occurs (green dashed line). Straight line indicates the spontaneous magnetization expected for the $Bi_{0.92}Nd_{0.08}Fe_{1-x}Mn_xO_3$ compounds upon removal of the cycloidal modulation.

ferromagnetic state in the $Bi_{0.86}La_{0.14-x}Sm_xFeO_3$ series coincides with the doping-induced ferroelectric-to-antiferroelectric transition.[39] This scenario common for the $Bi_{1-x}Ln_xFeO_3$ (Refs. 16, 20, 39, and 40) and $BiFe_{1-x}Mn_xO_3$ (Refs. 21 and 22) multiferroics is not found to be the case for the co-doped (Bi, Nd)$Fe_{1-x}Mn_xO_3$ (Fig. 5(a)). In this system, the change of the dominant magnetic state happens ahead of the polar-nonpolar structural phase transformation (green dashed region in Fig. 6). The situation is similar to that observed in the $Bi_{1-x}Ca_xFeO_3$,[32,43] $Bi_{1-x}Ca_xFe_{1-x}Ti_xO_3$,[43] and $Bi_{1-x}Ca_xFe_{1-x/2}Nb_{x/2}O_3$ (Ref. 43) series, where chemical substitution leading to a significant constriction of the initial unit cell volume favors stabilization of the weak ferromagnetic state within the rhombohedral ferroelectric phase. In the orthorhombic antiferroelectric phase (Fig. 5(b)), the room-temperature spontaneous magnetization and coercive field steadily decrease with increasing Mn content (blue solid region in Fig. 6). The behavior is consistent with a linear decrease of the Neel point observed in the $BiFe_{1-x}Mn_xO_3$ series that, in turn, correlates with changing the average number of e_g electrons on the B site.[21] A linear-like compositional dependence of the room-temperature spontaneous magnetization in the weak ferromagnetic antiferroelectric phase has also been found in the $Bi_{1-y}Pr_yFe_{1-x}Mn_xO_3$ ($y = 0.11$, 0.16; $x \leq 0.3$),[24] $Bi_{0.825}Nd_{0.175}Fe_{1-x}Mn_xO_3$ ($x \leq 0.3$),[25] and $Bi_{0.9}Sm_{0.1}Fe_{1-x}Mn_xO_3$ ($x \leq 0.4$)[26] perovskites, thus confirming a common trend characteristic of pure or lanthanide-modified $BiFeO_3$ upon Mn doping. The opposite situation is expected at low temperatures. Indeed, spontaneous magnetization in the $Bi_{0.825}Nd_{0.175}Fe_{1-x}Mn_xO_3$ series at $T = 5$ K increases with increasing manganese content.[25] Similar behavior is observed in the $LaFe_{1-y}Mn_yO_{3+\delta}$ system,[44,45] where competitive ferromagnetic (Mn^{3+}-O-Mn^{4+} and Mn^{3+}-O-Mn^{3+}) and antiferromagnetic (Fe^{3+}-O-Fe^{3+} and Fe^{3+}-O-Mn^{3+}) superexchange interactions[9,10] tend to stabilize the intermediate spin-glass-like state at low temperature. Extrapolation of the straight line drawn through the (x, M_s) points associated with the purely orthorhombic compounds ($x = 0.25$ and $x = 0.3$) passes through the point corresponding to the spontaneous magnetization of the structurally inhomogeneous $x = 0.2$ sample (thus indicating that the rhombohedral and orthorhombic wF phases possess very close spontaneous magnetization near the morphotropic phase boundary) and gives the "locked" magnetization of ~0.235 emu/g for the $Bi_{0.92}Nd_{0.08}FeO_3$ solid solution (Fig. 6). This magnetization should be released upon the field-induced removal of the cycloidal modulation; however, the magnetic field available in the experiment is not enough to accomplish the transition in the polycrystalline material (though a deviation from the linearity indicating a metamagnetic behavior starts to develop in the virgin $M(H)$ dependence above 40 kOe (i.e., in a good agreement with the recent H-x phase diagram proposed for the $Bi_{1-x}Nd_xFeO_3$ system[14])). In accordance with the previous observations made for the $Bi_{1-x}La_xFeO_3$ (Ref. 20) and $Bi_{1-x}Pr_xFeO_3$ (Ref. 16) series and suggesting a similar origin of weak ferromagnetism in the polar and nonpolar phases of the $BiFeO_3$-based compounds (namely, the Dzyaloshinsky-Moriya interaction[12]), the predicted value of the induced magnetization in $Bi_{0.92}Nd_{0.08}FeO_3$ is close to the spontaneous magnetization characteristic of the weak ferromagnetic state of the antiferroelectric $Bi_{1-x}Nd_xFeO_3$ perovskites.[41]

IV. CONCLUSIONS

Room-temperature X-ray diffraction, piezoresponse force microscopy, and SQUID-magnetometry measurements of the $Bi_{0.92}Nd_{0.08}Fe_{1-x}Mn_xO_3$ ($x \leq 0.3$) compounds were performed to illustrate effect of the B-site substitution on the crystal structure and multiferroic properties of the low-doped $Bi_{1-x}Ln_xFeO_3$ perovskites demonstrating a ferroelectric and dominant antiferromagnetic behaviors. It has been found that Mn doping suppresses the polar ionic displacements (thus decreasing spontaneous polarization from ~64 μC/cm^2 for $x = 0$ to ~53 μC/cm^2 for $x = 0.15$) and induces a ferroelectric-to-antiferroelectric transition at $x \sim 0.2$. A change of the dominant magnetic interaction is observed within the concentration region of the polar phase realization, so a weak ferromagnetic ferroelectric phase untypical of $Bi_{1-x}Ln_xFeO_3$ and $BiFe_{1-x}Mn_xO_3$ multiferroics is stabilized. Near the polar-nonpolar phase boundary, the parent rhombohedral and doping-induced orthorhombic phases possess the same spontaneous magnetization.

ACKNOWLEDGMENTS

This work was supported by funds from FEDER (Programa Operacional Factores de Competitividade COMPETE) and from FCT-Fundação para a Ciência e a Tecnologia under the project PEst-C/FIS/UI0036/2011, program "Ciência 2008", and grant SFRH/BPD/42506/2007.

FCT is also acknowledged for partial support within the project "Multifox" (PTDC/FIS/105416/2008).

[1]N. A. Hill, J. Phys. Chem. B **104**, 6694 (2000).
[2]W. Eerenstein, N. D. Mathur, and J. F. Scott, Nature **442**, 759 (2006).
[3]G. Catalan and J. F. Scott, Adv. Mater. **21**, 2463 (2009).
[4]J. B. Neaton, C. Ederer, U. V. Waghmare, N. A. Spaldin, and K. M. Rabe, Phys. Rev. B **71**, 014113 (2005).
[5]D. Lebeugle, D. Colson, A. Forget, and M. Viret, Appl. Phys. Lett. **91**, 022907 (2007).
[6]F. Kubel and H. Schmid, Acta Crystallogr., Sect. B: Struct. Sci. **46**, 698 (1990).
[7]A. Palewicz, I. Sosnowska, R. Przenioslo, and A. W. Hewat, Acta Phys. Pol. A **117**, 296 (2010).
[8]S. Picozzi and C. Ederer, J. Phys.: Condens. Matter **21**, 303201 (2009).
[9]J. B. Goodenough, Phys. Rev. **100**, 564 (1955).
[10]J. Kanamori, J. Phys. Chem. Solids **10**, 87 (1959).
[11]I. Sosnowska, T. Peterlin Neumaier, and E. Steichele, J. Phys. C **15**, 4835 (1982).
[12]I. Dzyaloshinsky, J. Phys. Chem. Solids **4**, 241 (1958); T. Moriya, Phys. Rev. **120**, 91 (1960).
[13]G. Le Bras, D. Colson, A. Forget, N. Genand Riondet, R. Tourbot, and P. Bonville, Phys. Rev. B **80**, 134417 (2009).
[14]P. Chen, O. Gunaydın Şen, W. J. Ren, Z. Qin, T. V. Brinzari, S. McGill, S. W. Cheong, and J. L. Musfeldt, Phys. Rev. B **86**, 014407 (2012).
[15]G. L. Yuan, S. W. Or, J. M. Liu, and Z. G. Liu, Appl. Phys. Lett. **89**, 052905 (2006); G. L. Yuan and S. W. Or, J. Appl. Phys. **100**, 024109 (2006).
[16]V. A. Khomchenko, I. O. Troyanchuk, D. V. Karpinsky, and J. A. Paixao, J. Mater. Sci. **47**, 1578 (2012).
[17]I. Levin, M. G. Tucker, H. Wu, V. Provenzano, C. L. Dennis, S. Karimi, T. Comyn, T. Stevenson, R. I. Smith, and I. M. Reaney, Chem. Mater. **23**, 2166 (2011).
[18]C. J. Cheng, D. Kan, S. H. Lim, W. R. McKenzie, P. R. Munroe, L. G. Salamanca Riba, R. L. Withers, I. Takeuchi, and V. Nagarajan, Phys. Rev. B **80**, 014109 (2009).
[19]D. A. Rusakov, A. M. Abakumov, K. Yamaura, A. A. Belik, G. Van Tendeloo, and E. Takayama Muromachi, Chem. Mater. **23**, 285 (2011).
[20]I. O. Troyanchuk, D. V. Karpinsky, M. V. Bushinsky, V. A. Khomchenko, G. N. Kakazei, J. P. Araujo, M. Tovar, V. Sikolenko, V. Efimov, and A. L. Kholkin, Phys. Rev. B **83**, 054109 (2011).
[21]S. M. Selbach, T. Tybell, M. A. Einarsrud, and T. Grande, Chem. Mater. **21**, 5176 (2009).
[22]A. A. Belik, A. M. Abakumov, A. A. Tsirlin, J. Hadermann, J. Kim, G. Van Tendeloo, and E. Takayama Muromachi, Chem. Mater. **23**, 4505 (2011).
[23]V. A. Khomchenko, I. O. Troyanchuk, D. V. Karpinsky, S. Das, V. S. Amaral, M. Tovar, V. Sikolenko, and J. A. Paixao, J. Appl. Phys. **112**, 084102 (2012).
[24]V. A. Khomchenko, I. O. Troyanchuk, M. I. Kovetskaya, M. Kopcewicz, and J. A. Paixao, J. Phys. D: Appl. Phys. **45**, 045302 (2012).
[25]V. A. Khomchenko, I. O. Troyanchuk, T. M. R. Maria, D. V. Karpinsky, S. Das, V. S. Amaral, and J. A. Paixao, J. Appl. Phys. **112**, 064105 (2012).
[26]V. A. Khomchenko, I. O. Troyanchuk, M. I. Kovetskaya, and J. A. Paixao, J. Appl. Phys. **111**, 014110 (2012).
[27]J. Bielecki, P. Svedlindh, D. T. Tibebu, S. Cai, S. G. Eriksson, L. Borjesson, and C. S. Knee, Phys. Rev. B **86**, 184422 (2012).
[28]S. Saxin and C. S. Knee, Dalton Trans. **40**, 3462 (2011).
[29]J. Rodríguez Carvajal, Physica B **192**, 55 (1993).
[30]A. M. Glazer, Acta Crystallogr., Sect. A: Cryst. Phys., Diffr., Theor., Gen. Crystallogr. **31**, 756 (1975).
[31]J. H. Lee, H. J. Choi, D. Lee, M. G. Kim, C. W. Bark, S. Ryu, M. A. Oak, and H. M. Jang, Phys. Rev. B **82**, 045113 (2010).
[32]V. A. Khomchenko, I. O. Troyanchuk, D. M. Tobbens, V. Sikolenko, and J. A. Paixao, J. Phys.: Condens. Matter **25**, 135902 (2013).
[33]J. Chaigneau, R. Haumont, and J. M. Kiat, Phys. Rev. B **80**, 184107 (2009).
[34]R. D. Shannon, Acta Crystallogr., Sect. A Cryst. Phys., Diffr., Theor. Gen. Crystallogr. **32**, 751 (1976).
[35]Y. M. Kim, A. Kumar, A. Hatt, A. N. Morozovska, A. Tselev, M. D. Biegalski, I. Ivanov, E. A. Eliseev, S. J. Pennycook, J. M. Rondinelli, S. V. Kalinin, and A. Y. Borisevich, Adv. Mater. **25**, 2497 (2013).
[36]D. Khomskii, Physics **2**, 20 (2009).
[37]A. K. Zvezdin and A. P. Pyatakov, Phys. Status Solidi B **246**, 1956 (2009).
[38]A. M. Kadomtseva, Yu. F. Popov, A. P. Pyatakov, G. P. Vorob'ev, A. K. Zvezdin, and D. Viehland, Phase Transitions **79**, 1019 (2006).
[39]V. A. Khomchenko, L. C. J. Pereira, and J. A. Paixao, J. Phys. D: Appl. Phys. **44**, 185406 (2011).
[40]I. O. Troyanchuk, M. V. Bushinsky, D. V. Karpinsky, O. S. Mantytskaya, V. V. Fedotova, and O. I. Prochnenko, Phys. Status Solidi B **246**, 1901 (2009).
[41]I. Levin, S. Karimi, V. Provenzano, C. L. Dennis, H. Wu, T. P. Comyn, T. J. Stevenson, R. I. Smith, and I. M. Reaney, Phys. Rev. B **81**, 020103 (2010).
[42]T. Shibata, B. Bunker, J. F. Mitchel, and P. Schiffer, Phys. Rev. Lett. **88**, 207205 (2002).
[43]I. O. Troyanchuk, M. V. Bushinsky, N. V. Tereshko, and M. I. Kovetskaya, JETP Lett. **93**, 512 (2011).
[44]O. F. de Lima, J. A. H. Coaquira, R. L. de Almeida, L. B. de Carvalho, and S. K. Malik, J. Appl. Phys. **105**, 013907 (2009).
[45]K. De, R. Ray, R. N. Panda, S. Giri, H. Nakamura, and T. Kohara, J. Magn. Magn. Mater. **288**, 339 (2005).